Spectral density analysis of nonlinear hysteretic systems

Mihai Dimian* and Isaak D. Mayergoyz
Department of Electrical and Computer Engineering and UMIACS, University of Maryland, College Park, Maryland 20742, USA
(Received 24 February 2004; published 28 October 2004)

A method for the analysis of spectral densities of hysteretic nonlinearities driven by diffusion processes is presented. This method is based on the Preisach formalism for the description of hysteresis and the mathematical machinery of diffusion processes on graphs. The calculations are appreciably simplified by the introduction of the "effective" distribution function. The implementation of the method for the case of the Ornstein-Uhlenbeck input process is presented in detail, and analytical expressions for spectral noise densities for various hysteretic systems are obtained. The general qualitative features of these spectral densities are examined and their dependence on various parameters is discussed. Because of the universality of the Preisach model, this approach can be used to compute spectra in hysteresis nonlinearities of various physical origins.

DOI: 10.1103/PhysRevE.70.046124 PACS number(s): 02.50.Ey, 75.60.Ej, 02.70.Uu, 74.40.+k

I. INTRODUCTION

The phenomenon of hysteresis has been known and has attracted the attention of many researchers for a long time. However, a systematic study of hysteresis was only recently attempted and led to the appearance of the first monographs on the subject [1–4]. Since then, interest in this topic has been continuously growing, and it has extended far beyond the classical areas of magnetism and plasticity. For example, optical hysteresis [5], superconducting hysteresis [6], and economic hysteresis [7] became well-established scientific domains, and many pioneering studies appeared in biology [8,9], psychology [10,11], and computer science [12,13].

The physical origin of hysteresis is due to the multiplicity of metastable states exhibited by hysteretic systems. A physical system can persist in a metastable state for some time, but thermal perturbations usually drive the system to more stable nearby states. In magnetism, this thermally activated relaxation is commonly called an "aftereffect" or "viscosity," while in the area of superconductivity it is known as "creep." Therefore, the behavior of a hysteretic system could be described as a nonlinear hysteretic transformation of a stochastic input that consists of a random internal noise superimposed on a deterministic external input. In other areas such as economics [7], computer science [12,13], or wireless communication [14], the external input of a hysteretic system is already considered as a stochastic process due to its random nature or to external noise. Regardless of the reasons that led to such models, the mathematical study of hysteretic systems driven by stochastic input is of relevance to all the previously mentioned areas. This point is also supported by the universality of the Preisach model that has been used to describe hysteretic nonlinearities of various physical origins. Furthermore, the study of multivalued nonlinear systems with stochastic inputs is still a hardly touched territory, being of considerable mathematical complexity [15]. Therefore, the techniques used to analyze the properties of these systems are of interest in their own right.

The calculation of spectral density is a central problem in physics. This problem is of considerable complexity for nonlinear physical systems and it has been studied in the past by such authorities in the field as van Vleck and Uhlenbeck. However, the calculation of spectra for hysteresis systems has not been attempted mainly because of the non-Markovian nature of the stochastic output processes. In this article, a method for computing spectral densities for complex hysteretic systems driven by diffusion processes is discussed, and computational results illustrating this method are presented. For the class of Ornstein-Uhlenbeck input processes, closed form (analytical) expressions for the spectral density are derived. The method takes full advantage of the fact that various hysteretic nonlinearities can be constructed through the Preisach formalism as a "weighted superposition" of rectangular loop operators that are individually driven by the same diffusion process. Then the mathematical theory of stochastic processes on graphs (see the Appendix) is used to circumvent the difficulties related to the fact that outputs of hysteretic systems are not Markovian processes. In addition, some special techniques are used to simplify the expression for the spectral density of output processes.

Preisach-type models with stochastic input were introduced by Mayergoyz and Kormann in [16–18] to offer a unified and detailed description of hysteresis and the aftereffect in magnetic materials [6,19–22]. Moreover, it has been shown that this approach can be successfully applied to the study of creep phenomena in type II superconductors [23] and in the fields of mechanical and structural engineering [24]. Key computations in these viscosity models are based on the relation between randomly induced switchings of rectangular loops and the exit problem for stochastic processes, which is a very well-studied problem in the theory of diffusion processes. Later, a simpler and more efficient technique for these computations was discovered, which uses the recently developed theory of diffusion processes on graphs [25]. This theory was first applied to the study of random perturbations of Hamiltonian dynamical systems [25,26]. Then it was realized that this mathematical technique is naturally suited for the analysis of noise in hysteretic systems [27,28].

*Electronic address: dimian@glue.umd.edu

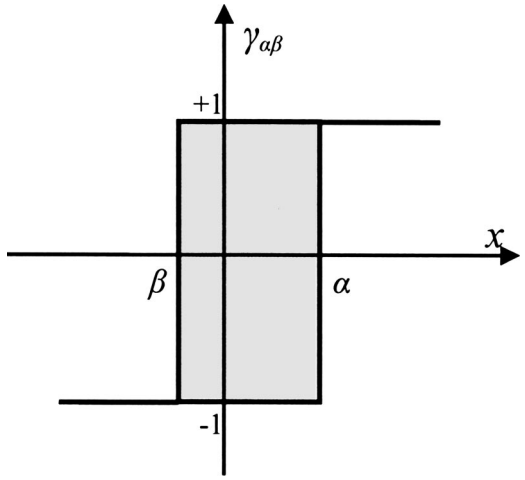

FIG. 1. Rectangular hysteresis loop that represents the operator $\hat{\gamma}_{\alpha\beta}$.

The article is organized as follows. In Sec. II, a general discussion of the method for the calculation of the spectral density of the output of the Preisach model driven by a diffusion process is presented. In Sec. III, this method is applied to the calculation of the spectral density in the case when the input is the Ornstein-Uhlenbeck process. Sample results of the computations of the spectral density and their analysis are presented in Sec. IV. Finally, conclusions are drawn in Sec. V.

II. DISCUSSION OF THE METHOD

Consider complex hysteretic nonlinearities that can be modeled through the Preisach formalism as weighted superpositions of rectangular loops. This can be mathematically described as follows:

$$h(t) = \int\int_{\alpha \geqslant \beta} \mu(\alpha,\beta)\hat{\gamma}_{\alpha\beta}x(t)d\alpha d\beta. \tag{1}$$

Here, $\mu(\alpha,\beta)$ is a Preisach distribution function, while $\hat{\gamma}_{\alpha\beta}$ are rectangular loop operators shown in Fig. 1. The Preisach model has been extensively used for the description of hysteresis of various physical types such as magnetic hysteresis [1–4], superconducting hysteresis [6,23], mechanical hysteresis of consolidated granular materials [29–31], hysteresis of shape-memory alloys [32] and piezoceramics [33], etc. This clearly revealed the physical universality of the Preisach model.

It has also been realized that the Preisach model driven by a stochastic input $x(t)$ is an effective model for thermally activated relaxations commonly known as the aftereffect in magnetism [16–22] and creep in the area of superconductivity [6,23]. The universality of this approach has made it naturally suitable for applications in the fields of mechanical and structural engineering, where the dynamic loading acting on hysteretic systems is usually random in nature [24]. It is expected that other areas where the input has a stochastic behavior, such as communications or economics, will benefit from this direction of research.

For many hysteretic materials (especially magnetic materials), the weight function $\mu(\alpha,\beta)$ is narrowly peaked around the line $\alpha=-\beta$. For these materials, the symmetric Preisach model constructed as a weighted superposition of symmetric rectangular loops $\hat{\gamma}_\alpha=\hat{\gamma}_{\alpha(-\alpha)}$ can be regarded as a fairly good approximation. This Preisach model can be written in the form

$$h(t) = \int_0^{\alpha_0} \hat{\gamma}_\alpha x(t)\mu(\alpha)d\alpha = \int_0^{\alpha_0} i_\alpha(t)\mu(\alpha)d\alpha, \tag{2}$$

where

$$i_\alpha(t) = \hat{\gamma}_\alpha x(t) = \begin{cases} 1 \text{ if } x(t) > \alpha, \\ -1 \text{ if } x(t) < -\alpha, \\ 1 \text{ if } x(t) \in (-\alpha,\alpha) \text{ and } x(\tau(t)) = \alpha, \\ -1, \text{if } x(t) \in (-\alpha,\alpha) \text{ and } x(\tau(t)) = -\alpha, \end{cases} \tag{3}$$

where $\tau(t)$ is the value of time at which the last threshold (α or $-\alpha$) was attained.

The input process $x(t)$ is assumed to be described by the Itô stochastic differential equation

$$dx(t) = b(x(t))dt + \sigma(x(t))dW(t), \tag{4}$$

with initial condition $x(0)=x_0$. Here $W(t)$ is the Wiener process, while b and σ are known functions that satisfy local Lipshitz and linear growth conditions [34–36]. These standard conditions ensure the existence of a nonexploding, unique solution of Eq. (4) that satisfies the initial condition.

The stochastic nature of the input leads to random switchings of the rectangular loop operators $\hat{\gamma}_\alpha$ and, therefore, the output of the Preisach model $h(t)$ is a stochastic process as well. The autocorrelation function of the output process is

$$\begin{aligned} C_h(\tau) &= \langle h(\tau)h(0)\rangle \\ &= \int_0^{\alpha_0}\int_0^{\alpha_0} \langle \hat{\gamma}_\beta x(\tau)\hat{\gamma}_\alpha x(0)\rangle \mu(\beta)\mu(\alpha)d\beta d\alpha, \end{aligned} \tag{5}$$

where $\langle\rangle$ denotes the expected value. Thus, we can express the autocorrelation of the Preisach model (2) as a weighted superposition of cross-correlation functions $C_{\beta\alpha}$ of two-dimensional processes $(i_\beta(t), i_\alpha(t))$, representing the outputs of two symmetric rectangular loops:

$$C_h(\tau) = \int_0^{\alpha_0}\int_0^{\alpha_0} C_{\beta\alpha}(\tau)\mu(\beta)\mu(\alpha)d\beta d\alpha. \tag{6}$$

The cross-correlation functions $C_{\beta\alpha}(\tau)$ are not even functions, but $C_{\beta\alpha}(-\tau)=C_{\alpha\beta}(\tau)$. This implies that the correlation function of the Preisach system $C_h(\tau)$ is an even function.

According to the Wiener-Khinchine theorem [36], the process's spectral density is the Fourier transform of the autocorrelation function. Because we deal with an even correlation function, the spectral density of the output process can be expressed as

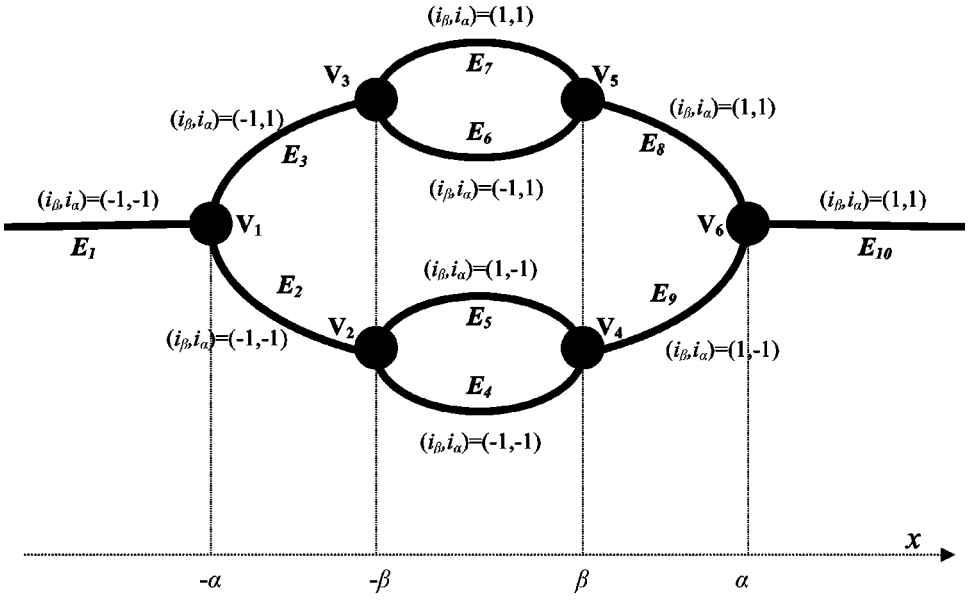

FIG. 2. Graph on which the three-component process **y** is defined.

$$S_h(\tau) = 2\ \mathrm{Re}\left\{\int_0^\infty C_h(\tau)e^{-j\omega\tau}d\tau\right\} = \int_0^{\alpha_0}\int_0^{\alpha_0} S_{\beta\alpha}(\omega)\mu(\beta)\mu(\alpha)d\beta d\alpha, \tag{7}$$

where $S_{\beta\alpha}(\omega)$ is the "cross-spectral density" for the two-dimensional process $(i_\beta(t), i_\alpha(t))$ and it is related to the cross-correlation function $C_{\beta a}(\tau)$ as follows:

$$S_{\beta\alpha}(\omega) = 2\ \mathrm{Re}\left\{\int_0^\infty C_{\beta\alpha}(\tau)e^{-j\omega\tau}d\tau\right\}. \tag{8}$$

The Preisach model describes hysteresis nonlinearities with nonlocal memories. For this reason, the output process $h(t)$ cannot be embedded as a component of some Markovian process. However, the previous expression shows that this spectral density can be expressed as a weighted superposition of spectral densities for much simpler processes $(i_\beta(t), i_\alpha(t))$. These processes are still non-Markovian, but they can be embedded in higher dimensional Markovian processes.

In order to compute $S_{\beta a}(\omega)$, we consider the three-component process $\mathbf{y}(t)=(i_\beta(t), i_\alpha(t), x(t))$, with $i_\alpha(t) = \hat{\gamma}_\alpha x(t)$, $i_\beta(t)=\hat{\gamma}_\beta x(t)$ defined on the graph Y shown in Fig. 2. Because the rectangular loop operators describe hysteresis with local memory, the joint specification of current values of input and output uniquely defines the states of this hysteresis. As a result, $\mathbf{y}(t)$ is a Markovian process. In addition, only certain combinations of $i_\beta(t), i_\alpha(t)$, and $x(t)$ are possible, and they are presented in Fig. 2. The binary processes $i_\beta(t)$ and $i_\alpha(t)$ assume constant values on the edges of the graph Y. Applying the theory of stochastic processes on graphs, the following initial-boundary value problem for the transition probability density function $\rho(\mathbf{y},t|\mathbf{y}',0)$ of the Markovian process $\mathbf{y}(t)$ defined on the graph Y can be derived (see the Appendix). On each edge of this graph, $\rho(\mathbf{y},t|\mathbf{y}',0)$ satisfies the forward Kolmogorov equation:

$$\frac{\partial\rho(\mathbf{y},t|\mathbf{y}',0)}{\partial t} + L_x\rho(\mathbf{y},t|\mathbf{y}',0) = 0, \tag{9}$$

where $\hat{L}_x$ is the second order elliptic operator associated with the input diffusion process defined in Eq. (4), and it is specified by the expression

$$\hat{L}_x\rho = -\frac{1}{2}\frac{\partial^2}{\partial x^2}[\sigma^2(x)\rho] - \frac{\partial}{\partial x}[b(x)\rho], \tag{10}$$

with $\sigma(x)$ and $b(x)$ being the diffusion and drift coefficients, respectively, of the input process $x(t)$. The function $\rho(\mathbf{y},t|\mathbf{y}',0)$ satisfies the initial conditions

$$\rho(\mathbf{y},0|\mathbf{y}',0) = \delta_{i_\beta i'_\beta}\delta_{i_\alpha i'_\alpha}\delta(x,x') \tag{11}$$

and it has to decay to zero as x goes to infinity. In addition, the so-called vertex type boundary conditions [6,28] at graph vertices have to be satisfied. These vertex type boundary conditions express the continuity of the transition probability density when the transition from one graph edge occurs without switching of the rectangular loop, and a zero boundary condition is imposed on the third graph edge connected to this vertex. Moreover, the probability current has to be conserved at each vertex. For example, at the vertex V_1 (corresponding to $x=-\alpha$, in the case $\alpha>\beta$), these conditions are explicitly written as

$$\rho((-1,-1,-\alpha^+),t|\mathbf{y}',0) = \rho((-1,-1,-\alpha^-),t|\mathbf{y}',0),$$

$$\rho((-1,1,-\alpha^+),t|\mathbf{y}',0) = 0,$$

$$\frac{\partial\rho}{\partial x}((-1,1,-\alpha^+),t|\mathbf{y}',0) + \frac{\partial\rho}{\partial x}((-1,-1,-\alpha^+),t|\mathbf{y}',0) = \frac{\partial\rho}{\partial x}((-1,-1,-\alpha^-),t|\mathbf{y}',0). \tag{12}$$

It is apparent that the stationary probability density of the process $\mathbf{y}(t)$ is the solution of the following boundary value problem:

$$\hat{L}_x \rho_s(\mathbf{y}) = 0 \text{ on each graph edge},$$

$$\lim_{x \to \pm\infty} \rho_s(\mathbf{y}) = 0.$$

vertex boundary conditions at each graph vertex. (13)

Taking into account the facts presented above, the cross-correlation function $C_{\beta a}(\alpha)$ can be seen as a component of the correlation matrix $\mathbf{C}_\mathbf{y}(\tau)$ for the Markovian process $\mathbf{y}(t)$:

$$\begin{aligned}\mathbf{C}_\mathbf{y}(\tau) &= \langle \mathbf{y}^T(\tau)\mathbf{y}(0)\rangle \\ &= \int_{-\infty}^{\infty}\int_{-\infty}^{\infty} \sum_{i_\alpha, i_\beta} \sum_{i'_\alpha, i'_\beta} \mathbf{y}^T \mathbf{y}' \rho(\mathbf{y}, \tau; \mathbf{y}', 0) dx dx' \\ &= \int_{-\infty}^{\infty}\int_{-\infty}^{\infty} \sum_{i_\alpha, i_\beta} \sum_{i'_\alpha, i'_\beta} \mathbf{y}^T \mathbf{y}' \rho(\mathbf{y}, \tau | \mathbf{y}', 0) \rho_s(\mathbf{y}') dx dx'.\end{aligned} \tag{14}$$

In the above formula, the sums are taken over all graph values of the (i_β, i_α) and (i'_β, i'_α), respectively. This convention is maintained throughout the paper.

To simplify the computation of the cross-correlation function, the "effective" distribution function $g(\mathbf{y}, \tau)$ is introduced:

$$g(\mathbf{y}, \tau) = \int_{-\infty}^{\infty} \sum_{i'_\alpha, i'_\beta} i'_\alpha \rho(\mathbf{y}, \tau | \mathbf{y}', 0) \rho_s(\mathbf{y}') dx'. \tag{15}$$

A similar function has been previously proposed in [37] and used in the analysis of noise in semiconductor devices.

By using Eq. (9) on each edge of the graph, the initial condition (11), and vertex type boundary conditions for the transition probability density $\rho(\mathbf{y}, t | \mathbf{y}', 0)$, as well as the boundary value problem (13) for the stationary probability density $\rho_s(\mathbf{y}')$, one can derive the following initial boundary value problem for the "effective" distribution function:

$$\frac{\partial g(\mathbf{y}, \tau)}{\partial \tau} + L_x g(\mathbf{y}, \tau) = 0 \text{ on each graph edge},$$

$$g(\mathbf{y}, 0) = i_\alpha \rho_s(\mathbf{y}),$$

$$\lim_{x \to \pm\infty} g(\mathbf{y}, \tau) = 0,$$

vertex boundary conditions. (16)

Using formulas (14) and (15) the cross-correlation function $C_{\beta\alpha}(\tau)$ can be expressed by the formula

$$C_{\beta\alpha}(\tau) = \int_{-\infty}^{\infty} \sum_{i_\alpha, i_\beta} i_\beta g((i_\beta, i_\alpha, x), \tau) dx. \tag{17}$$

Thus, in order to find the cross-correlation function $C_{\beta a}(\tau)$, one has to solve first the boundary value problem (13) for the stationary distribution $\rho_s(\mathbf{y})$ and then the initial boundary value problem (16) for the "effective" distribution function $g(\mathbf{y}, \tau)$, and finally to compute the integral (17). According to Eq. (8), another integration has to be performed for the computation of the cross-spectral density $S_{\beta\alpha}(\omega)$. However, by introducing the one-side Fourier transform of the "effective" distribution function,

$$G(\mathbf{y}, \omega) = \int_0^\infty g(\mathbf{y}, \tau) e^{-j\omega\tau} d\tau, \tag{18}$$

the cross-spectral density $S_{\beta\alpha}(\omega)$ can be written in the form

$$S_{\beta\alpha}(\omega) = 2 \text{ Re}\left\{ \int_0^\infty \sum_{i_\alpha, i_\beta} i_\beta G(\mathbf{y}, \omega) dx \right\}. \tag{19}$$

Performing the Fourier transformation of the initial boundary value problem (16), we arrive at the following boundary value problem for $G(\mathbf{y}, \omega)$:

$$j\omega G(\mathbf{y}, \omega) + L_x G(\mathbf{y}, \omega) = i_\alpha \rho_s(\mathbf{y}) \text{ on each graph edge},$$

$$\lim_{x \to \pm\infty} G(\mathbf{y}, \omega) = 0,$$

vertex boundary conditions. (20)

For example, these "vertex" boundary conditions at the vertex $V_1(x = -\alpha)$ are

$$G((-1, -1, -\alpha^+), \omega) = G((-1, -1, -\alpha^-), \omega),$$

$$G((-1, 1, -\alpha^+), \omega) = 0,$$

$$\frac{\partial G}{\partial x}((-1, 1, -\alpha^+), \omega) + \frac{\partial G}{\partial x}((-1, -1, -\alpha^+), \omega) = \frac{\partial G}{\partial x}((-1, -1, -\alpha^-), \omega). \tag{21}$$

Because the stationary probability distribution satisfies the differential equation of the boundary value problem (13), the function $(i_\alpha / j\omega)\rho_s(\mathbf{y})$ is (for each ω) a particular solution for the nonhomogeneous differential equation in (20). Taking into account the linearity of the operator L_x, $G(\mathbf{y}, \omega)$ can be written as

$$G(\mathbf{y}, \omega) = G^0(\mathbf{y}, \omega) + \frac{i_\alpha}{j\omega} \rho_s(\mathbf{y}), \tag{22}$$

where $G^0(\mathbf{y}, \omega)$ is a solution of the corresponding homogeneous equation. Since the particular solution is purely imaginary, it does not contribute to the cross-spectral density $S_{\beta\alpha}(\omega)$. Thus,

$$S_{\beta\alpha}(\omega) = 2 \text{ Re}\left\{ \int_0^\infty \sum_{i_\alpha, i_\beta} i_\beta G^0(\mathbf{y}, \omega) dx \right\}, \tag{23}$$

with $G^0(\mathbf{y}, \omega)$ satisfying the following boundary value problem:

$$j\omega G^0(\mathbf{y}, \omega) + L_x G^0(\mathbf{y}, \omega) = 0 \quad \text{on each graph edge},$$

$$\lim_{x\to\pm\infty} G^0(\mathbf{y},\omega) = 0,$$

inhomogeneous vertex type boundary conditions. (24)

Next, we describe these inhomogeneous vertex type boundary conditions. First, by inspecting vertex boundary conditions for $G(\mathbf{y},\omega)$ and $\rho_s(\mathbf{y})$, it can be observed that, when a transition from one edge to another occurs without switching of the rectangular loops, $G(\mathbf{y},\omega)$ and $\rho_s(\mathbf{y})$ corresponding to these edges are continuously matched and i_α does not change its value. Consequently, the corresponding $G^0(\mathbf{y},\omega)$ is also continuously matched in this case. On the third edge connected to the vertex, the zero boundary condition is valid. Until this point, the inhomogeneous vertex boundary type conditions coincide with the previous ones. This coincidence is also maintained in the boundary conditions for derivatives at vertices $V_{2-5}(x=\pm\beta)$. However, the difference appears in the conditions for derivatives at vertices V_1 and $V_6(x=\pm\alpha)$; namely, from the boundary condition (21) for the derivative of $G(\mathbf{y},\omega)$, we have

$$\begin{aligned}&\frac{\partial G^0}{\partial x}((-1,1,-\alpha^+),\omega)+\frac{1}{j\omega}\frac{\partial \rho_s}{\partial x}(-1,1,-\alpha^+)\\&\quad+\frac{\partial G^0}{\partial x}((-1,-1,-\alpha^+),\omega)+\frac{(-1)}{j\omega}\frac{\partial \rho_s}{\partial x}(-1,-1,-\alpha^+)\\&=\frac{\partial G^0}{\partial x}((-1,-1,-\alpha^-),\omega)+\frac{(-1)}{j\omega}\frac{\partial \rho_s}{\partial x}(-1,-1,-\alpha^-).\end{aligned} \tag{25}$$

Taking into account the boundary condition for a stationary probability distribution, the following boundary condition for $G^0(\mathbf{y},\omega)$ is derived:

$$\begin{aligned}&\frac{\partial G^0}{\partial x}((-1,1,-\alpha^+),\omega)+\frac{\partial G^0}{\partial x}((-1,-1,-\alpha^+),\omega)\\&\quad+\frac{2}{j\omega}\frac{\partial \rho_s}{\partial x}(-1,1,-\alpha^+)\\&=\frac{\partial G^0}{\partial x}((-1,-1,-\alpha^-),\omega).\end{aligned} \tag{26}$$

By using similar arguments, the inhomogeneous vertex boundary condition at the vertex V_6 is found to be

$$\begin{aligned}&\frac{\partial G^0}{\partial x}((1,1,\alpha^-),\omega)+\frac{\partial G^0}{\partial x}((1,-1,\alpha^-),\omega)-\frac{2}{j\omega}\frac{\partial \rho_s}{\partial x}(1,-1,\alpha^-)\\&=\frac{\partial G^0}{\partial x}((1,1,\alpha^+),\omega).\end{aligned} \tag{27}$$

In the case $\alpha<\beta$, the boundary conditions for vertices corresponding to $x=\mp\alpha$ take the following forms:

$$\begin{aligned}&\frac{\partial G^0}{\partial x}((i_\beta,1,\mp\alpha^\pm),\omega)+\frac{\partial G^0}{\partial x}((i_\beta,-1,\mp\alpha^\pm),\omega)\\&\quad\pm\frac{2}{j\omega}\frac{\partial \rho_s}{\partial x}(i_\beta,\pm1,\mp\alpha^\pm)\\&=\frac{\partial G^0}{\partial x}((i_\beta,\mp1,\mp\alpha^\mp),\omega).\end{aligned} \tag{28}$$

Now the method for the computation of the spectral density can be summarized as the sequence of the following steps.

Step 1. Solve the boundary value problem (13) for the stationary distribution $\rho_s(\mathbf{y})$.

Step 2. Solve the boundary value problem (24) for $G^0(\mathbf{y},\omega)$.

Step 3. Compute the cross-spectral density $S_{\beta\alpha}(\omega)$ by using formula (23).

Step 4. Compute the spectral density $S_h(\omega)$ by using formula (7).

The following observations can simplify the implementation of the above steps.

(1) For a given input, the first three steps of the method are independent of the Preisach function $\mu(\alpha)$. Therefore, once the $S_{\beta\alpha}(\omega)$ are precomputed, they can be used for any "symmetric" Preisach system (2). In other words, the spectral density of a hysteretic system can be computed as a weighted superposition of cross-spectral densities $S_{\beta\alpha}(\omega)$ precomputed at the third step, with the weight being given by the Preisach function of that system.

(2) As can be observed from Eq. (23), the cross-spectral densities $S_{\beta\alpha}(\omega)$ are expressed as linear combinations of $G^0(\mathbf{y},\omega)$ corresponding to different edges. This indicates that it may not be necessary to find an explicit expression for $G^0(\mathbf{y},\omega)$ on every edge, but rather their linear combinations mentioned above.

(3) By using the expression (10) for the operator $\hat{L}_x$, an important simplification can be made. From formula (24) it follows that $G^0(\mathbf{y},\omega)=(j/\omega)\hat{L}_x G^0(\mathbf{y},\omega)$. By substituting the latter expression into formula (23), one can obtain

$$\begin{aligned}S_{\beta\alpha}(\omega)&=2\ \mathrm{Re}\left\{\int_0^\infty \sum_{i_\alpha i_\beta} i_\beta\left(\frac{j}{\omega}\right)\hat{L}_x G^0(\mathbf{y},\omega)dx\right\}\\&=-\frac{2}{\omega}\mathrm{Im}\left\{\int_0^\infty \hat{L}_x\left(\sum_{i_\alpha i_\beta} i_\beta G^0(\mathbf{y},\omega)\right)dx\right\}.\end{aligned} \tag{29}$$

The derivatives in the operator $\hat{L}_x$ can be integrated and this results in a simple expression for the spectral density in terms of the first derivatives of $G^0(\mathbf{y},\omega)$ at vertex points [see, for example, Eq. (41)].

(4) The boundary value problems (23) and (24) defined on the entire graph Y can be sequentially reduced to the boundary value problems defined on real line intervals, which are more tractable analytically and numerically. Efficient numerical algorithms for solving these problems defined on the real line interval are three-diagonal matrix solvers described, for instance, in Ref. [38].

The above observations produce further simplifications in the method for computations of the spectral density once a specific form of the input stochastic process is given. These advantages will be further exploited in the next section, where the Ornstein-Uhlenbeck process is used as a model of driving noise.

The proposed method is conceptually valid for Preisach systems with nonsymmetric rectangular loops, although the algorithmic complexity of computations will be appreciably increased.

III. HYSTERETIC SYSTEMS DRIVEN BY THE ORNSTEIN-UHLENBECK PROCESS

In this section we shall apply the method developed in the previous section to the case when the input is an Ornstein-Uhlenbeck (OU) process and analytical expressions for the spectral density will be obtained. As was discussed in the Introduction, the stochastic nature of the input in hysteresis systems is generally due to (internal or external) noise superimposed on the external deterministic input. It is natural to require the stochastic process that models the noise to be a stationary Gaussian Markovian process. According to the Doob theorem [35], the only process that satisfies these requirements is the OU process. This noise model is used in a wide class of physical systems [36,39] and has a very interesting history that was described by Nelson in [40].

For an OU process, the operator $\hat{L}_x$ has the form

$$\hat{L}_x f = -\frac{\sigma^2}{2}\frac{\partial^2 f}{\partial x^2} - b\frac{\partial[(x-x_0)f]}{\partial x}. \tag{30}$$

Next, we shall discuss how the steps 1 through 4 can be implemented for this case and analytical expressions will be derived. As a result, closed form expressions for the spectral densities of hysteretic systems driven by OU input noise are found.

Step 1

For the OU process, the boundary value problem (13) for the stationary distribution of the process $\mathbf{y}(t)$ defined on the graph Y was solved in [27] and the results are

$$\rho_s(\mathbf{y}) = \begin{cases} \tilde{\rho}_s(x) & \text{on } E_1 \text{ and } E_{10}, \\ \tilde{\rho}_s(x)[1-\varphi_{-\alpha\alpha}(x)] & \text{on } E_2 \text{ and } E_8, \\ \tilde{\rho}_s(x)\varphi_{-\alpha\alpha}(x) & \text{on } E_3 \text{ and } E_9, \\ \tilde{\rho}_s(x)[1-\varphi_{-\alpha\alpha}(x)][1-\varphi_{-\beta\beta}(x)] & \text{on } E_4, \\ \tilde{\rho}_s(x)[1-\varphi_{-\alpha\alpha}(x)]\varphi_{-\beta\beta}(x) & \text{on } E_5, \\ \tilde{\rho}_s(x)\varphi_{-\alpha\alpha}(x)[1-\varphi_{-\beta\beta}(x)] & \text{on } E_6, \\ \tilde{\rho}_s(x)\varphi_{-\alpha\alpha}(x)\varphi_{-\beta\beta}(x) & \text{on } E_7, \end{cases} \tag{31}$$

where

$$\tilde{\rho}_s(x) = \sqrt{\frac{b}{\pi\sigma^2}}e^{-b(x-x_0)^2/\sigma^2}, \tag{32}$$

$$\varphi_{a_1a_2}(x) = \frac{\int_{a_1}^{x} e^{b(y-x_0)^2/\sigma^2}}{\int_{a_1}^{a_2} e^{b(y-x_0)^2/\sigma^2}}. \tag{33}$$

The results for the case $\alpha<\beta$ are obtained by interchanging α and β, as well as i_α and i_β.

Step 2

Next, the boundary value problem (24) defined on the graph Y is reduced to boundary value problems defined on line intervals, which are more tractable both analytically and numerically. This technique is very useful because it could be applied to steps 1 and 2 of the method in the case of a general input diffusion process (4). The resulting boundary value problems defined on the line intervals can be solved numerically by using three-diagonal matrix solvers [38].

First, we formulate the boundary value problem for $G^0(x,\omega)=\Sigma_{i_\alpha i_\beta}G^0(\mathbf{y},\omega)$, where the sum is taken over all graph edges:

$$j\omega G^0(x,\omega) + L_x G^0(x,\omega) = 0, \quad x \in (-\infty,+\infty)\setminus\{-\alpha,\alpha\},$$

$$\lim_{x\to\pm\infty} G^0(x,\omega) = 0,$$

$$\frac{\partial G^0}{\partial x}(-\alpha^-,\omega) - \frac{\partial G^0}{\partial x}(-\alpha^+,\omega) = \frac{2}{j\omega}\sqrt{\frac{b}{\pi\sigma^2}}\frac{1}{\int_{-\alpha}^{\alpha} e^{b(y-x_0)^2/\sigma^2}},$$

$$\frac{\partial G^0}{\partial x}(\alpha^-,\omega) - \frac{\partial G^0}{\partial x}(\alpha^+,\omega) = -\frac{2}{j\omega}\sqrt{\frac{b}{\pi\sigma^2}}\frac{1}{\int_{-\alpha}^{\alpha} e^{b(y-x_0)^2/\sigma^2}}. \tag{34}$$

The solution to this problem coincides with the solution of problem (24) for edges E_1 and E_{10}. In addition, it will also help to simplify the expression for the cross-spectral density.

Second, we formulate the boundary value problem for $G^0(1,x,\omega)=\Sigma_{i_\beta}G^0((1,i_\beta,x),\omega)$, where the sum is taken over "central" graph edges. In the case $\alpha<\beta$, $G^0(1,x,\omega)=\Sigma_{i_\alpha}G^0((i_\alpha,1,x),\omega)$.

From formulas (24) and (31), we find

$$j\omega G^0(1,x,\omega) + L_x G^0(1,x,\omega) = 0, \quad x \in (-\alpha,\alpha),$$

$$G^0(1,-\alpha,\omega) = 0,$$

$$G^0(1,\alpha,\omega) = G^0(\alpha,\omega) \tag{35}$$

for the case of $\alpha>\beta$ and

$$j\omega G^0(1,x,\omega) + L_x G^0(1,x,\omega) = 0, \quad x \in (-\beta,\beta)\setminus\{-\alpha,\alpha\},$$

$$G^0(1,-\beta,\omega) = 0,$$

$$G^0(1,\beta,\omega) = G^0(\beta,\omega),$$

$$\frac{\partial G^0}{\partial x}(1,\alpha^-,\omega)-\frac{\partial G^0}{\partial x}(1,\alpha^+,\omega)=-\frac{2}{j\omega}\sqrt{\frac{b}{\pi\sigma^2}}\frac{\varphi_{-\beta\beta}(\alpha)}{\int_{-\alpha}^{\alpha}e^{b(y-x_0)^2/\sigma^2}}$$

$$\frac{\partial G^0}{\partial x}(1,-\alpha^-,\omega)-\frac{\partial G^0}{\partial x}(1,-\alpha^+,\omega)$$
$$=\frac{2}{j\omega}\sqrt{\frac{b}{\pi\sigma^2}}\frac{\varphi_{-\beta\beta}(-\alpha)}{\int_{-\alpha}^{\alpha}e^{b(y-x_0)^2/\sigma^2}} \tag{36}$$

for the case of $\alpha<\beta$.

It is obvious that $G^0(-1,x,\omega)=G^0(x,\omega)-G^0(1,x,\omega)$ in both cases. The solutions of these problems coincide with the solution of the problem (24) for the edges E_2, E_3 and E_8, E_9. To completely solve the problem (24), one should find the solution for the "central" edges E_{4-7}. However, it will be shown below that the cross-spectral density can be expressed in terms of the previously found functions, and, consequently, the solution of problem (24) for these "central" edges is not necessary. Thus, the boundary value problem (24) defined on the entire graph Y was reduced to the boundary value problems defined on line intervals.

In the case of an OU input process, the specific form of the operator $\hat{L}_x$ is helpful in order to find an explicit analytical solution to the problem (24) in terms of parabolic cylinder functions; namely, one can observe that if a function $\tilde{f}$ satisfies the differential equation for the parabolic cylinder functions

$$\frac{\partial^2\tilde{f}}{\partial\tilde{x}^2}(\tilde{x},\omega)+\left[-\frac{1}{4}\tilde{x}^2+\left(\frac{1}{2}-j\frac{\omega}{b}\right)\right]\tilde{f}(\tilde{x},\omega)=0, \tag{37}$$

then the function $f(x,\omega)=\tilde{f}(\sqrt{2b(x-x_0)}/\sigma,\omega)e^{-b(x-x_0)^2/2\sigma^2}$ represents a solution to the differential equation

$$j\omega f(x,\omega)+\hat{L}_x f(x,\omega)=0, \tag{38}$$

with $\hat{L}_x$ defined by Eq. (30). Let f_1 and f_2 be the solutions of Eq. (38) corresponding to parabolic cylinder functions that vanish at $+\infty$ and $-\infty$, respectively [41]. The solution to the problem (24) on each graph edge can be expressed as a linear combination of these functions:

$$G^0(\mathbf{y},\omega)=\lambda_1(i_1,i_2,\omega)f_1(x,\omega)+\lambda_2(i_1,i_2,\omega)f_2(x,\omega). \tag{39}$$

The coefficients $\lambda_1(i_1,i_2,\omega)$ and $\lambda_2(i_1,i_2,\omega)$ corresponding to each edge are found (for a given frequency) by matching the inhomogeneous "vertex" boundary conditions of the problem (24) (for that frequency). Thus, the analytical expression for the solution of the problem (24) can be expressed in terms of parabolic cylinder functions. In addition to having importance in its own right, the analytical approach described can be used to test the accuracy of numerical techniques applicable for a general nonexplosive diffusion input.

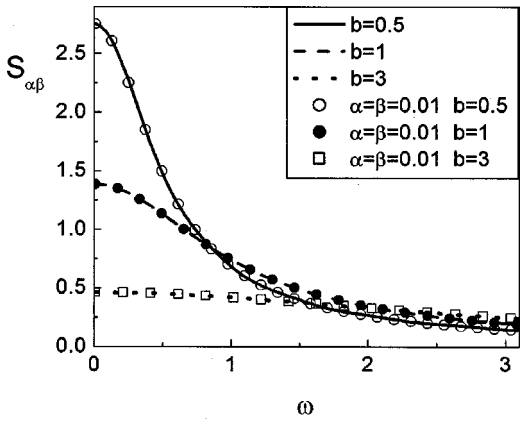

FIG. 3. Spectral density for a hard limiter system using analytical formula (44) (lines) and spectral density $S_{\beta\alpha}(\beta=\alpha=0.01)$ computed using the presented method (symbols) for selected values of the drift coefficient b.

Step 3

Using observation 3 from Sec. II, the cross-spectral density $S_{\beta\alpha}(\omega)$ can be expressed as

$$S_{\beta\alpha}(\omega)=-\frac{2}{\omega}\mathrm{Im}\left\{\int_{-\infty}^{\infty}\frac{\sigma^2}{2}\frac{\partial^2\left(\sum_{i_\alpha,i_\beta}i_\beta G^0\right)}{\partial x^2}-b\frac{\partial\left((x-x_0)\sum_{i_\alpha,i_\beta}i_\beta G^0\right)}{\partial x}dx\right\}. \tag{40}$$

The derivatives in Eq. (40) can be integrated and appropriate vertex boundary conditions can be used in the simplification of Eq. (40). By using formulas (24) and (31)–(36), one can derive the following formula for the cross-spectral density, for $\alpha<\beta$:

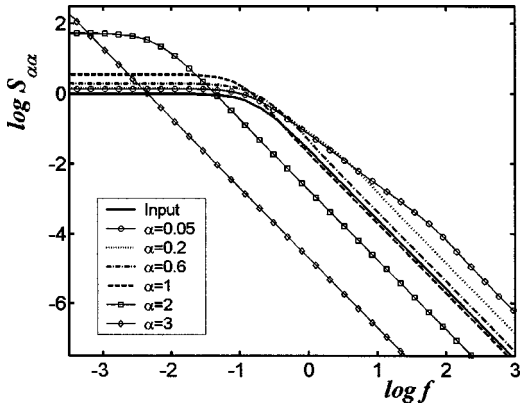

FIG. 4. Spectral density $S_{\alpha\alpha}$ of a rectangular loop for various widths of the loop α plotted on a $\log_{10}$-$\log_{10}$ scale. The Ornstein-Uhlenbeck input parameters are $b=\sigma=1$, $x_0=0$.

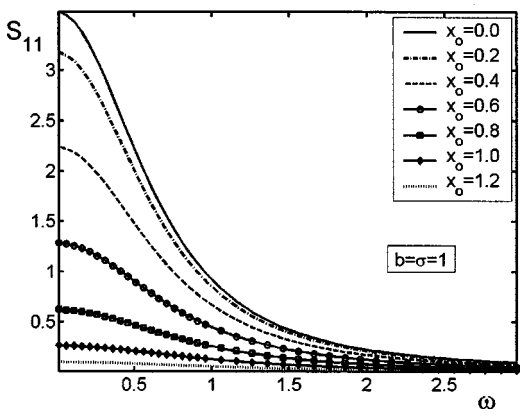

FIG. 5. Spectral density S_{11} for various values of the input average value $x_0(b=\sigma=1)$.

$$S_{\beta\alpha}(\omega)=\frac{4\sigma\sqrt{b}}{\omega^2\sqrt{\pi}\int_{-\beta}^{\beta}e^{b(y-x_0)^2/\sigma^2}dy}-\frac{2\sigma^2}{\omega}\mathrm{Im}\left[\frac{\partial G^0}{\partial x}(1,-\beta^+,\omega)-\frac{\partial G^0}{\partial x}(1,\beta^-,\omega)+\frac{\partial G^0}{\partial x}(\beta^+,\omega)\right], \tag{41}$$

while for $\alpha>\beta$ we have

$$S_{\beta\alpha}(\omega)=\frac{4\sigma\sqrt{b}}{\omega^2\sqrt{\pi}\int_{-\alpha}^{\alpha}e^{b(y-x_0)^2/\sigma^2}dy}-\frac{2\sigma^2}{\omega}\mathrm{Im}\left\{\sum_{i_\alpha}\left[\frac{\partial G^0}{\partial x}(1,i_\alpha,-\beta^+,\omega)-\frac{\partial G^0}{\partial x}(1,i_\alpha,\beta^-,\omega)\right]+\frac{\partial G^0}{\partial x}(\beta^+,\omega)\right\}. \tag{42}$$

According to Eq. (39), $G^0(\mathbf{y},\omega)$ can be represented in terms of parabolic cylinder functions on each graph edge and, consequently, an explicit analytical formula in terms of parabolic cylinder functions can be given for the cross-spectral density $S_{\beta\alpha}(\omega)$.

Step 4

Using formulas (41) and (42) for cross-spectral densities $S_{\beta\alpha}(\omega)$ in Eq. (7) and taking into account the relation (39), a closed form expression for the spectral density for the output process of a Preisach system characterized by a distribution μ and driven by an OU process is found.

IV. COMPUTATIONAL RESULTS AND THEIR DISCUSSION

In this section, we present and analyze the computational results for various hysteretic systems driven by OU processes. As has already been mentioned in Sec. II (observation 1), the calculation of cross-spectral densities $S_{\beta\alpha}(\omega)$ is independent of the choice of the Preisach distribution μ. Therefore, once computed, $S_{\beta\alpha}(\omega)$ can be used for any Preisach system (2) as long as the same input process is considered for these systems. The spectral density of the output process $S_h(\omega)$ is then constructed as a weighted superposition of cross-spectral densities $S_{\beta\alpha}(\omega)$ with weights given by the Preisach distribution [see Eq. (7)]. These observations entitle us to discuss the properties of the function $S_{\beta\alpha}(\omega)$.

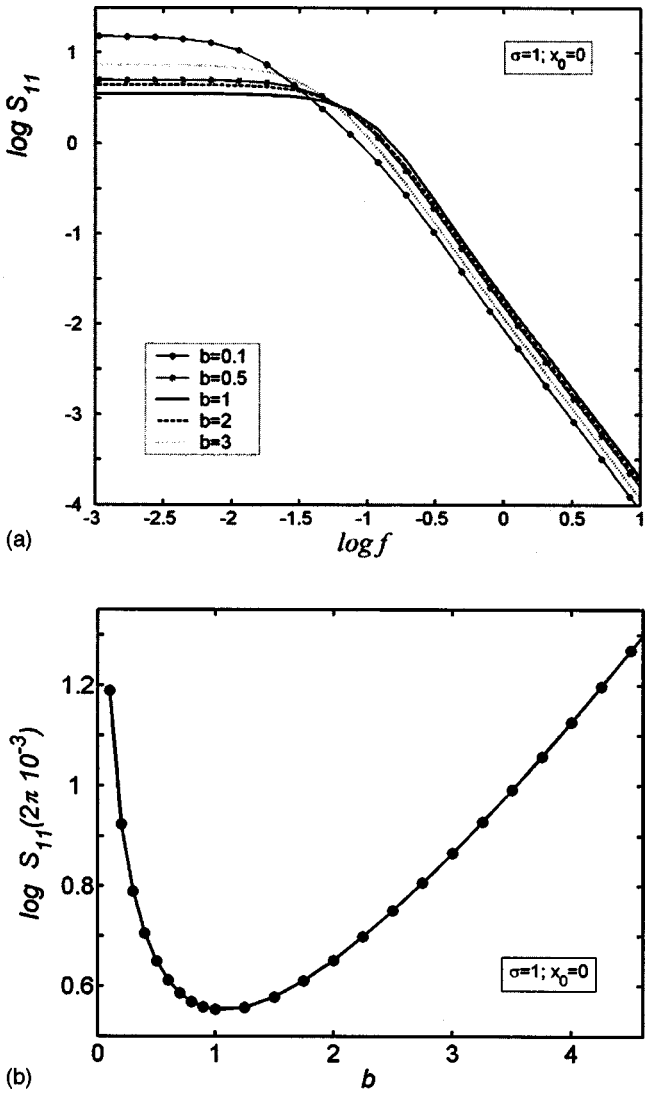

FIG. 6. (a) Spectral density S_{11} for selected values of the drift coefficient b plotted on a $\log_{10}$-$\log_{10}$ scale ($\sigma=1, x_0=0$). (b) Magnitude of S_{11} in the white noise region plotted against b.

As a test of our method, we have compared our results with the classical ones obtained for a hard limiter (strong clipping) system. These results can be traced back to the work of van Vleck [42,43]. It has been shown that the autocorrelation of the output of a hard limiter is related to the autocorrelation of the input by the so-called arcsine law

$$C_{HL}(\tau)=\frac{2}{\pi}\arcsin\frac{C_x(\tau)}{C_x(0)}. \tag{43}$$

In the case when the input is an OU process, the spectral density of the output is given by the formula

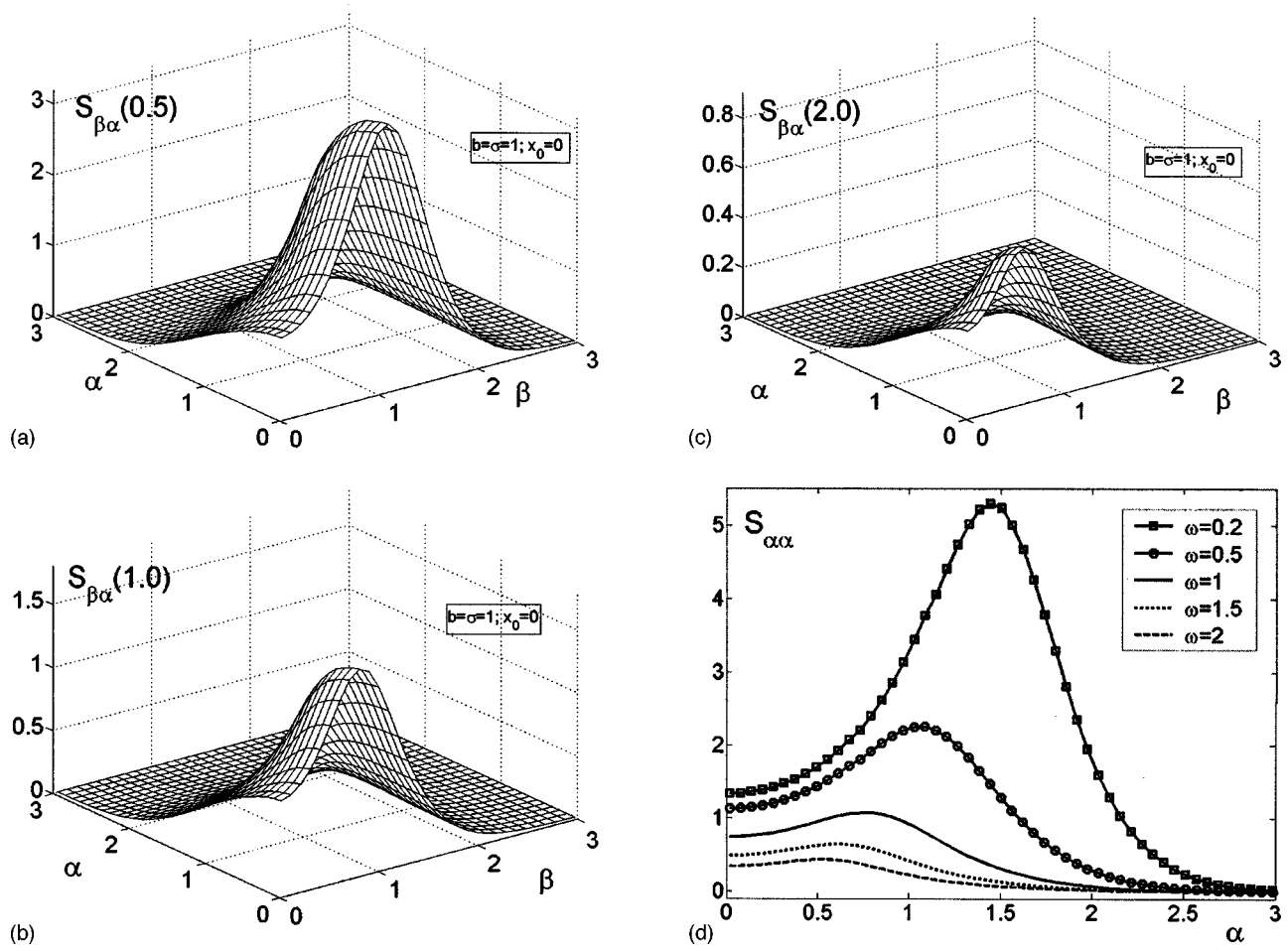

FIG. 7. (a)–(c) Variation of cross spectral density $S_{\beta\alpha}$ with respect to the widths β and α of the two loops, for $\omega=0.5$ (a), 1 (b), and 2 (c). (d) Diagonal sections $S_{\alpha\alpha}$ plotted for different frequencies $f(\omega=2\pi f)$.

$$S_{HL}(\omega)=\frac{4}{\pi}\int_0^\infty \arcsin(e^{-bt})\cos(\omega t)dt. \tag{44}$$

It is clear that the function $S_{\alpha\alpha}(\omega)$ represents the spectral density of the output of a rectangular loop $\hat{\gamma}_\alpha$. When the width of the loop approaches zero, the rectangular loop operator $\hat{\gamma}_\alpha$ approaches the step operator corresponding to a hard limiter system. As a consequence, the function $S_{\alpha\alpha}(\omega)$ should converge to $S_{HL}(\omega)$ if α tends to zero. In Fig. 3, some sample results of the comparison between the function $S_{\alpha\alpha}(\omega)$ computed by using our method and the function $S_{HL}(\omega)$ given by the formula (44) are presented. It is apparent from Fig. 3 that $S_{\alpha\alpha}(\omega)$ practically coincides with $S_{HL}(\omega)$ for sufficiently small α.

Next, we examine the influence of the input parameters and system characteristics on the spectral density $S_{\alpha\alpha}(\omega)$ of the output of a rectangular loop. In addition to being interesting in its own right, this analysis will be also useful for understanding the behavior of the function $S_{\beta\alpha}(\omega)$ and, implicitly, that of the spectral density $S_h(\omega)$ of a Preisach system. In Fig. 4, the dependence of the spectral noise density on the loop width is presented. For narrow loops, the spectral noise density is similar to that of a step operator (hard limiter system) where the region of the white noise is connected to the region of $1/f^2$ noise through an intermediate region of $1/f^\alpha$ behavior (the frequency $f=\omega/2\pi$). As can be seen from Fig. 4, the intermediate frequency region is reduced as the loop is broadened, and the variations of the loop width lead mostly to self-similar transformations of the spectral noise density graph. Another interesting observation that emerges from this analysis is related to the transformation of the spectral band. It is known that memoryless nonlinearities broaden spectral bands. However, memory effects may lead to the opposite results, as is evident from Fig. 4. By analyzing the formula for $S_{\alpha\alpha}(\omega)$ and the related boundary value problems, the following scaling property can be deduced:

$$S_{\alpha\alpha}((x_0,b,\sigma),\omega)=\left(\frac{\alpha}{\sigma}\right)^2 S_{11}\left(\left[\frac{x_0}{\alpha},b\left(\frac{\alpha}{\sigma}\right)^2,1\right],\omega\left(\frac{\alpha}{\sigma}\right)^2\right). \tag{45}$$

The advantage provided by formula (45) is that the computation of the spectral density for various OU inputs and various widths of the loop is reduced to the computation of the spectral density S_{11} for various external inputs x_0 and the drift coefficient b. The effect of an external deterministic input x_0 (an applied magnetic field, for instance) can be seen

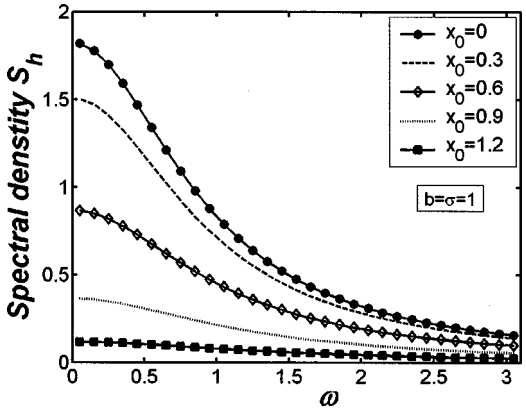

FIG. 8. Spectral density S_h for a hysteretic system with uniform type Preisach distribution for different values of input average value $x_0(b=\sigma=1)$.

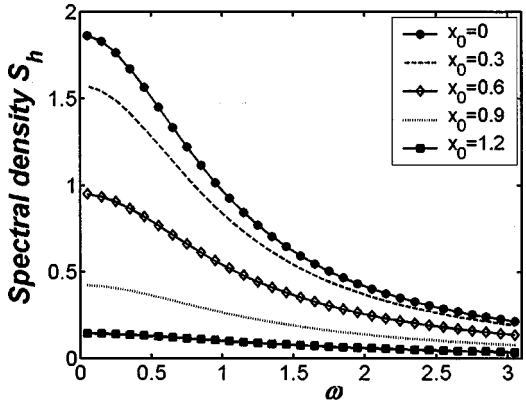

FIG. 9. Spectral density S_h for a hysteretic system with Gaussian type Preisach distribution for different values of input average value $x_0(b=\sigma=1)$.

from Fig. 5. It is apparent that when x_0 is increased output signals "stabilize" around +1 and, consequently, the spectral noise density is diminished. In Fig. 6(a), sample results of the computation of the spectral density S_{11} for selected values of the drift coefficient b are presented. The magnitude of the spectral density in the white noise region is plotted against the drift coefficient b in Fig. 6(b).

Next, consider an OU input process with $b=\sigma=1$ and $x_0=0$ (no external field applied). In Figs. 7(a)–7(c), variations of the cross-spectral density $S_{\beta\alpha}(\omega)$ with respect to the widths β and α of the two loops are presented for some selected values of the frequency. The cross-spectral density has negligible values outside a finite region around the origin, and this region becomes smaller when the frequency is increased. For a better understanding of the relation between the graphs presented in Figs. 7(a)–7(c), the diagonal section $[S_{\alpha\alpha}(\omega)]$ is plotted in Fig. 7(d) for different frequencies. It can be clearly observed that the maximum of $S_{\alpha\alpha}(\omega)$ becomes more pronounced and it is shifted toward "wider loops" as the frequency is decreased. This suggests that two Preisach systems whose Preisach distributions coincide near the origin should have approximately the same spectral noise densities for high frequencies. It is apparent that the region in the (β,α) plane that gives the main contribution to the spectral density depends on the characteristics of the input. It is also expected that $S_{\beta\alpha}(\omega)$ will decrease for every β and α as x_0 is shifted from zero.

The computations suggest that $S_{\beta\alpha}(\omega)$ undergoes monotonic variations with respect to ω for fixed β and α. This observation leads to the conclusion that the spectral noise density of a Preisach system driven by an OU process should be a decreasing function of frequency, regardless of the shape of the Preisach distribution.

As has been stressed, once $S_{\beta\alpha}(\omega)$ is computed, the calculation of the spectral noise density for any Preisach system (2) is reduced to the integration of this function with some specific weight related to the Preisach distribution [see Eq. (7)]. First, we considered a uniform Preisach distribution $\mu(\alpha)=1, \alpha\in(0,1)$. The results of computations for some selected values of the external deterministic input x_0 and the OU noise characterized by $b=\sigma=1$ are shown in Fig. 8. The same spectral analysis is shown in Fig. 9 for the case of a Gaussian type μ distribution. It can be observed that the Gaussian type distribution leads to higher spectral densities than the uniform one. As is expected, these hysteretic systems have a monotonic spectral density, and an increase in the external deterministic input x_0 (applied field) results in a decrease in the output noise spectrum.

V. CONCLUSION

A method for the calculation of spectral densities for hysteretic systems driven by diffusion processes is presented. The outputs of such systems are non-Markovian processes that represent nonlinear hysteretic transformations of diffusion processes. For this reason, the calculation of their spectral densities is associated with considerable mathematical difficulties. The method proposed in this paper circumvents these difficulties by using the Preisach description of hysteretic systems as well as the recently developed theory of diffusion processes on graphs. In addition, special techniques are used to simplify the expression for the spectral density of the output process. The case of Ornstein-Uhlenbeck input noise is extensively discussed, and the spectral noise densities of various Preisach systems are obtained. The Ornstein-Uhlenbeck input process is of special physical significance as a model of noise because of its stationary, Gaussian, and Markovian nature. Moreover, the closed form expressions for spectra have been obtained in this case. The general qualitative features of these spectral densities are examined and their dependence on various parameters is elucidated. Because of the universality of the Preisach model, the method developed is useful for the calculation of spectra in hysteretic systems of various physical types.

APPENDIX: DIFFUSION PROCESSES ON GRAPHS

The theory of stochastic processes on a graph has been recently developed by Freidlin and Wentzell [25]. This theory was first applied to the study of random perturbations of Hamiltonian dynamical systems [25,26]. Then it was realized that this mathematical technique is naturally suitable

for the analysis of noise in hysteretic systems [27,28,44]. In this appendix, we give a short description of diffusion processes on a graph based on the previously cited references. This description is adapted to our problem. Finally, the initial boundary value problem (9)–(12) for the transition probability density of the Markovian process $\mathbf{y}(t)$ is derived.

Consider a connected graph Y with vertices $V_1,\ldots,V_m$ and edges $E_1,\ldots,E_n$. Several edges can meet at a vertex V_k; we will write $E_j \sim V_k$ if the edge E_j has the vertex V_k as its end. With each edge E_j, a diffusion process $x^j(t)$ is associated that is governed by the second order elliptic operator

$$T = b(x)\frac{\partial}{\partial x} + \frac{\sigma^2(x)}{2}\frac{\partial^2}{\partial x^2}. \tag{A1}$$

Here, b and σ satisfy local Lipschitz and linear growth conditions (see [34,35]) and $\sigma(x) > c > 0$. We will denote by A_Y the infinitesimal operator of a strongly continuous semigroup of linear operators on the space $C(Y)$ of continuous functions corresponding to a Markov process $\mathbf{y}(t)$ on the graph Y with a continuous path.

The immediate task is to characterize the behavior of the diffusion process at the interior vertices of the graph Y. It has been shown in [25] that for any continuous Markov process $\mathbf{y}(t)$ on Y that is governed by the operator T inside E_j one can find nonnegative constants α_k and χ_{kj}, with $\alpha_k + \Sigma_{j:E_j \sim V_k} \chi_{kj} > 0$ for $k=1,\ldots,m$, such that the infinitesimal operator A_Y of that process is defined for any function f from $C(Y)$ that satisfies the following conditions.

(1) f is twice continuously differentiable inside the edges E_j.

(2) If $E_j \sim V_k$ then $\lim_{\mathbf{y}\to V, \mathbf{y}\in E_j} Tf(\mathbf{y})$ exists and is independent of j; this limit will be denoted by $Tf(V_k)$.

(3) $\alpha_k Tf(V_k) + \Sigma_{j:E_j \sim O_k} \chi_{kj} (\partial f/\partial y_j)(V_k) = 0$ for $k=1,\ldots,m$, where y_j is the coordinate on E_j equal to the distance of the point of E_j from V_k.

These conditions at the vertices will be further called "gluing" conditions. The constants α_k describe how much time the process spends in V_k, and the constants χ_{kj} are (roughly speaking) proportional to the probabilities that the process will "move" from vertex V_k along the edges E_j. For the model presented in Sec. II (see Fig. 2), the following facts can be established. Since the process has no delay at the vertices, $\alpha_k = 0$ for $k=1,\ldots,6$. Moreover, it is clear that in our case there is zero probability that the process $\mathbf{y}(t)$ will move from vertex V_2 along the edge E_3, while random motions along the edges E_1 and E_2 are equally probable. Therefore, $\chi_{13}=0, \chi_{11}=\chi_{12}=1$. Taking into account that the coordinates $y_1 = -\alpha - x$ and $y_2 = -\alpha + x$, we arrive at the following interface condition at the vertex V_1:

$$\frac{df_{E_1}}{dx}(-\alpha) = \frac{df_{E_2}}{dx}(-\alpha). \tag{A2}$$

Similar assertions are valid for each interior vertex, and analogous interface conditions can be derived.

The next task is to specify the partial differential equations for the transition probability density $\rho(t,\mathbf{y}|\mathbf{y}',0)$ corresponding to the Markov process $\mathbf{y}(t)$. Since $\mathbf{y}(t) = (i_\beta(t), i_\alpha(t), x(t))$ and the binary processes $i_\beta(t)$ and $i_\alpha(t)$ assume constant values on each edge E_k, the following notation for the transition probability density is justified:

$$\rho^{(j)}(t,x|\mathbf{y}',0) = \rho(t,\mathbf{y}|\mathbf{y}',0)_{\mathbf{y}\in E_j}. \tag{A3}$$

According to the theory of Markovian processes, the following equality is valid for $\rho^{(j)}$:

$$\sum_{j=1}^{10} \int_{E_j} f \frac{\partial \rho^{(j)}}{\partial t} dx = \sum_{j=1}^{10} \int_{E_j} (Tf)\rho^{(j)} dx. \tag{A4}$$

By integrating by parts in the equality (A3) and taking into account the interface conditions presented above and the fact that f can be chosen arbitrary in the domain of the infinitesimal operator A_Y, one finds that the transition probability density $\rho(t,\mathbf{y}|\mathbf{y}',0)$ satisfies the forward Kolmogorov equation (9) and the vertex boundary conditions (12).

[1] M. A. Krasnoselskii and A. V. Pokrovskii, *Systems with Hysteresis* (Springer, Berlin, 1989).

[2] I. D. Mayergoyz, *Mathematical Models of Hysteresis* (Springer, New York, 1991).

[3] A. Visintin, *Differential Models of Hysteresis* (Springer, Berlin, 1994).

[4] M. Brokate and J. Sprekels, *Hysteresis and Phase Transitions* (Springer, New York, 1996).

[5] N. N. Rosanov, *Spatial Hysteresis and Optical Patterns* (Springer, Berlin, 2002).

[6] I. D. Mayergoyz, *Mathematical Models of Hysteresis and Their Applications* (Elsevier, New York, 2003).

[7] *The Handbook of Economics Methodology*, edited by J. B. Davis, D. Wade Mans, and U. Maki (Edward Elgor, Cheltenham, 1998).

[8] F.-Y. Li, J.-M. Yuan, and G.-Y. Mou, Phys. Rev. E **70**, 021905 (2001).

[9] L. D. S. L. Strenberg, Global Ecol. Biogeogr. **10**, 369 (2001).

[10] P. Kruse, H. O. Carmesin, L. Pahlke, D. Struber, and M. Stadler, ZKW Ber. **3/96**, 1 (1996).

[11] *Memory for Everyday and Emotional Events*, edited by L. Stein, P. A. Orstein, B. Tversky, and C. Brainerd (Lawerence Erlbaum Associates, New Jersey, 1997).

[12] O. I. Ibe and J. Keilson, Perform. Eval. **21**, 185 (1995).

[13] N. Seelam, P. Sethi, and W. Feng, in *Management of Multimedia on the Internet*, Lecture Notes in Computer Science Vol. 2216 (Springer-Verlag, Heidelberg, 2001), p. 1.

[14] *Future Mobile Networks: 3G and Beyond*, edited by A. Clapton (IEE, London, 2001).

[15] *Unsolved Problems of Noise and Fluctuations*, edited by D. Abbott and L. B. Kish, AIP Conf. Proc. No. 511 (AIP, Melville, NY, 2000).

[16] I. D. Mayergoyz and C. E. Korman, J. Appl. Phys. **69**, 2128 (1991).
[17] I. D. Mayergoyz and C. E. Korman, IEEE Trans. Magn. **27**, 4766 (1991).
[18] I. D. Mayergoyz and C. E. Korman, J. Appl. Phys. **75**, 5478 (1994).
[19] C. E. Korman and P. Rugkwamsook, IEEE Trans. Magn. **33**, 4176 (1997).
[20] P. Rugkwamsook, C. E. Korman, G. Bertotti, and M. Pasquale, J. Appl. Phys. **85**, 4361 (1999).
[21] R. A. Fry, A. Reimars, L. H. Bennet, and E. Della Torre, Physica B **275**, 50 (2000).
[22] V. Basso, C. Beatrice, M. LoBue, P. Tiberto, and G. Bertotti, Phys. Rev. B **61**, 1278 (2000).
[23] I. D. Mayergoyz, A. A. Adly, M. W. Huang, and C. Kraft, IEEE Trans. Magn. **36**, 3208 (2000).
[24] Z. G. Ying, W. Q. Zhu, Y. Q. Ni, and J. M. Ko, J. Sound Vib. **254**, 37 (2002).
[25] M. I. Freidlin and A. D. Wentzell, Ann. Prob. **21**, 2215 (1993).
[26] M. I. Freidlin, *Markov Processes and Differential Equations: Asymptotic Problems* (Springer, Berlin, 1996).
[27] M. I. Freidlin, I. D. Mayergoyz, and R. Pfeiffer, Phys. Rev. E **62**, 1850 (2000).
[28] I. D. Mayergoyz and M. Dimian, J. Appl. Phys. **93**, 6826 (2003).
[29] R. A. Guyer, K. R. McCall, and G. N. Boitnott, Phys. Rev. Lett. **74**, 3491 (1995).
[30] R. A. Guyer, J. TenCate, and P. A. Johnson, Phys. Rev. Lett. **82**, 3280 (1999).
[31] R. A. Guyer and P. A. Johnson, Phys. Today **52**(4), 30 (1999).
[32] K. Wilmanski, Int. J. Eng. Sci. **31**, 1121 (1993).
[33] P. Ge and M. Jouaneh, Precis. Eng. **17**, 211 (1995).
[34] B. Oksendal, *Stochastic Differential Equations* (Springer, Berlin, 1995).
[35] I. I. Gihman and A. V. Skorohod, *Stochastic Differential Equations* (Springer, Berlin, 1972).
[36] C. Gardiner, *Handbook of Stochastic Methods for Physics, Chemistry and the Natural Sciences* (Springer, Berlin, 2002).
[37] C. E. Korman and I. D. Mayergoyz, Phys. Rev. B **54**, 17620 (1996).
[38] I. S. Berezin and N. P. Zhidkov, *Computing Methods* (Pergamon, Oxford, 1965).
[39] J. L. Lawson and G. E. Uhlenbeck, *Threshold Signals* (Dover, New York, 1965).
[40] E. Nelson, *Dynamical Theories of Brownian Motion* (Princeton University Press, Princeton, NJ, 1967).
[41] *Handbook of Mathematical Functions*, edited by M. Abramowitz and I. Stegun (Dover, New York, 1971).
[42] A. Papoulis, *Probability, Random Variables and Stochastic Processes* (McGraw-Hill, New York, 1984).
[43] J. H. van Vleck, RRL Report No. 51, 1943 (unpublished).
[44] R. M. Pfeiffer, Ph.D. thesis, University of Maryland, 1998.